RadioGraphics

CT in Nontraumatic Acute Thoracic Aortic Disease: Typical and Atypical Features and Complications[1]

Eva Castañer, MD • Marta Andreu, MD • Xavier Gallardo, MD
Josep Maria Mata, MD, PhD • María Ángeles Cabezuelo, MD
Yolanda Pallardó, MD

ONLINE-ONLY CME

See www.rsna.org/education/rg_cme.html.

LEARNING OBJECTIVES

After reading this article and taking the test, the reader will be able to:

- Recognize the various conditions that might cause clinical symptoms similar to those of aortic dissection.
- Identify the CT findings in typical aortic dissection, intramural hematoma, and penetrating atherosclerotic ulcer.
- Describe the potential complications of aortic dissection and their appearances at CT.

Thoracic aortic dissection is the most frequent cause of aortic emergency, and unless it is rapidly diagnosed and treated, the result is death. Helical computed tomography (CT) permits the diagnosis of acute aortic dissection with a sensitivity and specificity of nearly 100%. This imaging modality also enables differentiation between proximal aortic dissection (type A in the Stanford classification) and distal aortic dissection (Stanford type B), which are treated differently and have different prognoses. In 70% of patients in whom nontraumatic acute thoracic aortic dissection is diagnosed after evaluation with helical CT, scans show the typical signs of aortic dissection, with rupture and displacement of the intima. CT also can depict other pathologic entities with similar clinical manifestations, such as intramural hematoma and penetrating atherosclerotic ulcer. Awareness of the different radiologic appearances of these disease entities is essential for differential diagnosis. More than one-third of patients with aortic dissection show signs and symptoms indicative of systemic involvement. Because branch-vessel involvement may increase morbidity and mortality, in this group of patients it is important to evaluate the entire aorta so as to determine the distal extent of the dissection and detect any systemic involvement.

Abbreviation: IMH = intramural hematoma

Index terms: Aorta, stenosis or obstruction, 56.151 • Aorta, CT, 56.1211

RadioGraphics 2003; 23:S93–S110 • **Published online** 10.1148/rg.23si035507

[1]From the Departments of Radiology (E.C., M.A., X.G., J.M.M.) and Pathology (M.A.C.), SDI UDIAT-CD, Institut Universitari Parc Taulí-UAB, Corporació Parc Taulí, Parc Taulí s/n, 08208 Sabadell, Spain; and Department of Radiology, Hospital de la Ribera, Alzira, Spain (Y.P.). Recipient of a Certificate of Merit award for an education exhibit at the 2002 RSNA scientific assembly. Received February 7, 2003; revision requested April 16 and received May 27; accepted June 11. **Address correspondence to** E.C. (e-mail: *ecastaner@cspt.es*).

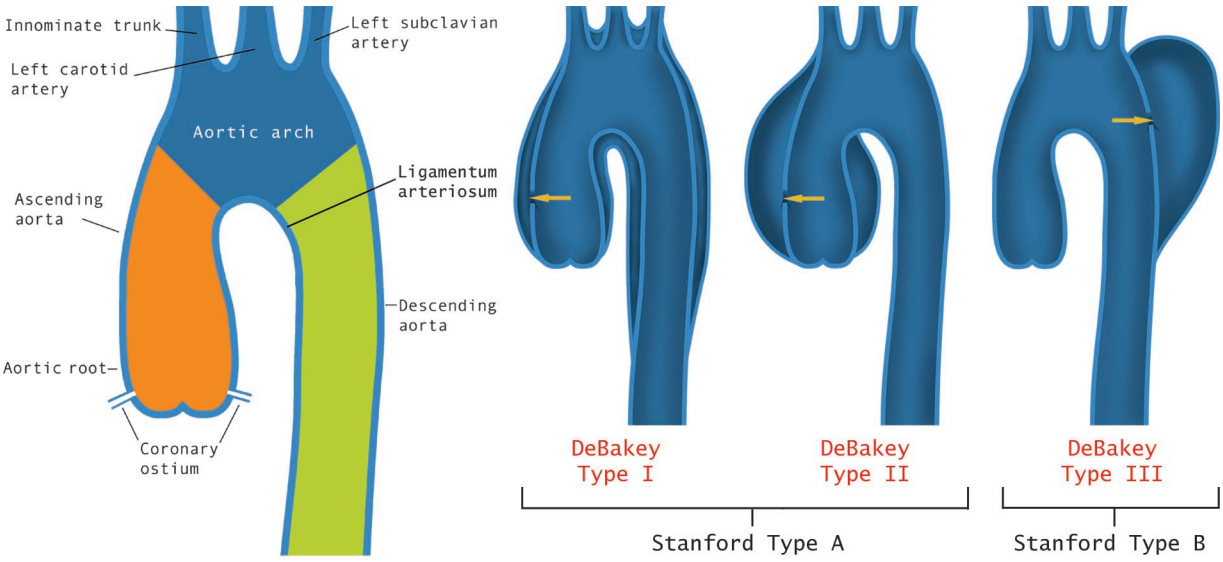

a. b.

Figure 1. **(a)** Diagram of the thoracic aorta shows the ascending segment, transverse segment or arch, and descending segment, which begins distal to the ligamentum arteriosum. On CT scans, the landmark that indicates the beginning of the descending aorta is the left subclavian artery. **(b)** Drawing shows the Stanford classifications of aortic dissections and the equivalent DeBakey classifications.

Introduction

Acute thoracic aortic dissection is a life-threatening condition that requires immediate diagnosis and treatment. Acute aortic dissection is the most common cause of aortic emergency. Its prevalence exceeds that of thoracoabdominal aortic aneurysm rupture (1).

Computed tomography (CT), because of its speed and its wide availability, is currently the most common diagnostic imaging method for the study of acute aortic dissection. Helical CT enables the diagnosis of acute aortic dissection with a sensitivity and specificity of nearly 100% (2,3). CT scans in 70% of cases of acute aortic dissection depict an intimal flap. CT also is useful for identifying atypical forms of dissection, such as intramural hematoma (IMH) and penetrating atherosclerotic ulcer. These three entities are clinically indistinguishable; all may produce chest or back pain in a patient with hypertension. CT also enables the evaluation of other thoracoabdominal structures. A thorough assessment is especially important to detect possible complications of aortic dissection, such as ischemic and obstructive diseases, which can increase morbidity and mortality.

Thoracic aortic dissection may be described as acute or chronic, depending on its clinical manifestation. Dissection is considered acute if the symptoms last less than 2 weeks and chronic if they last longer (4). Seventy-five percent of deaths from the condition occur within 2 weeks after the initial manifestation of symptoms (5). In addition, dissection is classified according to the extent of involvement of the thoracic aorta. The original system for classification of aortic dissection, the DeBakey system, has been superseded by the Stanford system, which includes two types based on whether surgery is required (6). Dissection affecting the ascending aorta or the aortic arch (Fig 1a, 1b) is classified as Stanford type A (DeBakey types I and II) (6,7) and accounts for 75% of cases of aortic dissection. Acute type A dissection should be repaired immediately to avoid fatal complications, such as extension to the pericardium, the pleural space, the coronary arteries, or the aortic valvular ring. Chronic proximal dissection, also classified as Stanford type A, is usually associated with medial layer anomalies (eg, cystic medial necrosis), and it too must be surgically treated. Acute dissection that begins distal to the left subclavian artery is classified as Stanford type B (DeBakey type III). The patient affected by Stanford type B dissection is treated medically for hypertension unless complications occur (eg, abdominal organ ischemia or persistent pain) that indicate a progression of the dissection and, eventually, the need for surgery.

The classic signs of typical aortic dissection depicted at CT are rupture and displacement of the intima. However, atypical dissections caused by IMH and penetrating atherosclerotic ulcer may manifest similar signs. Recognition of the complications that often accompany aortic dissection is important for achieving accurate diagnosis and effective treatment. In this article, we show imaging findings in typical and atypical aortic dissections and describe their differentiation.

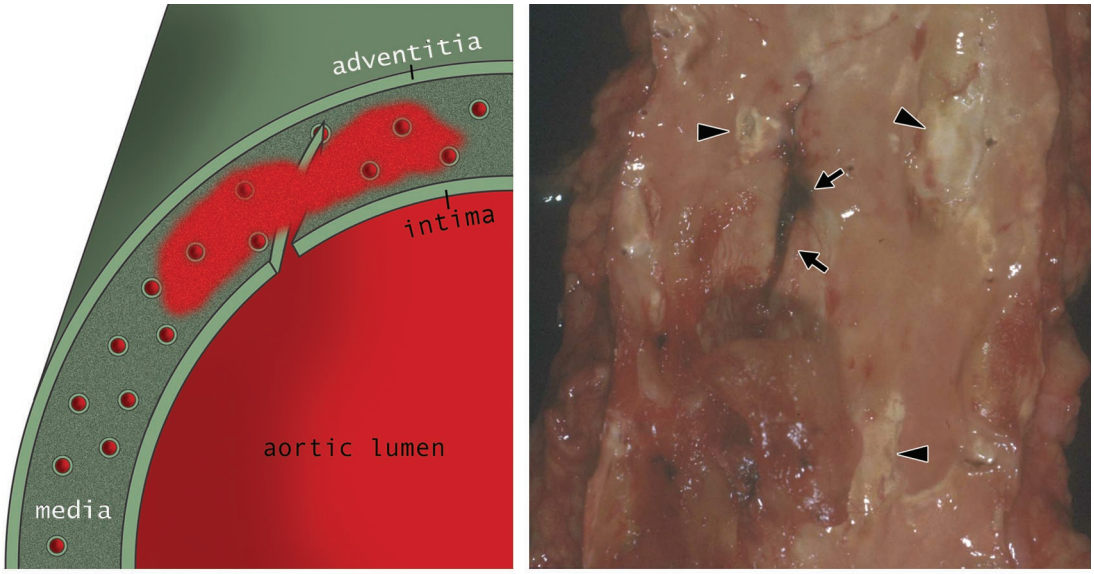

a. b.

Figure 2. **(a)** Schematic of aortic layers in typical aortic dissection shows a tear of the intimal layer, which has resulted in the formation of two lumina (one false, one true). **(b)** Photograph of an autopsy specimen shows a Stanford type B aortic dissection. An intimal tear (arrows) and intimal calcifications (arrowheads) are clearly visible in the descending aorta.

In describing the appearance of aortic dissection at CT, we distinguish between features observed on CT scans obtained with contrast material enhancement and those observed on scans obtained without contrast material enhancement. When acute aortic dissection is suspected, unenhanced CT scans should always be obtained to detect IMH. It is important to evaluate the entire aorta so as to determine the distal extent of the dissection and to detect ischemic disease.

Imaging Technique

At our institution, helical CT examinations are performed with a single-detector scanner with a 0.75-second rotation time. The examination begins with the acquisition of an unenhanced CT scan. Images are obtained with a table feed of 10 mm, collimation of 7 mm, and reconstruction increment of 7 mm. Coverage begins 3 cm above the aortic arch and continues to the upper side of the femoral head. Unenhanced CT scans are useful for diagnosing IMH and acute hemorrhage (pleural, pericardial, or mediastinal).

After unenhanced CT, contrast-enhanced CT is performed with a bolus injection of 120 mL of nonionic contrast material at a rate of 3 mL/sec through a 21-gauge catheter. The catheter should be positioned in the right arm, if possible, to avoid opacification of the left brachiocephalic vein, which could result in a perivenous artifact that substantially degrades visualization of the origin of the brachiocephalic artery. We use a scanning delay of 25 seconds. In general, optimal imaging of the thoracic aorta and abdominal aorta is obtained with scanning delays of 20–30 and 30–40 seconds, respectively. Enhanced CT is performed with the following parameters: 190 mA, 120 kV, pitch of 1.5, 5-mm collimation, and 3- or 5-mm reconstruction increment. Coverage begins 3 cm above the aortic arch and continues to the bifurcation of the iliac artery.

Helical CT is the most common initial diagnostic test performed when acute aortic dissection is suspected. Because of the wide availability of helical CT and because it enables rapid diagnosis in emergent situations, in many institutions helical CT is the method of choice for evaluating the aorta in acute situations. Most magnetic resonance (MR) imagers have limited capability for depiction of acute aortic disease and are used mostly for evaluation of patients with stable or chronic aortic conditions. One advantage of MR imaging over CT is the ability of the former to depict complications such as left ventricular dysfunction and valvular regurgitation (7,8). The recently developed 8- and 16-element multidetector CT scanners enable coverage of the entire aorta, from the valve to the femoral heads, in 20–30 seconds of scanning time and with 1-mm section thickness. The new imagers undoubtedly will further increase the accuracy of CT for detection of aortic disease.

Typical Aortic Dissection

Typical aortic dissection is produced by an intimal tear that allows blood to enter the medial layer, giving rise to two lumina, one true and one false (Fig 2).

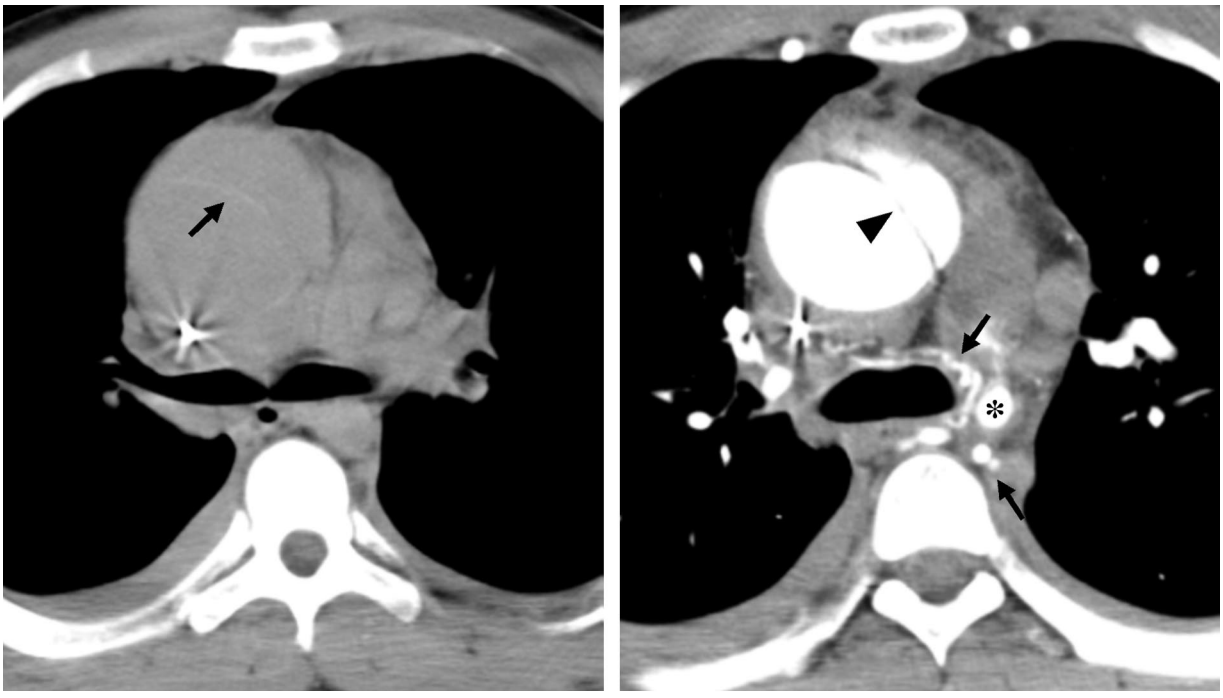

a. b.

Figure 3. Rupture of a Stanford type A typical aortic dissection in an 18-year-old patient with aortic coarctation. **(a)** Unenhanced CT scan shows an aneurysm and displaced intima in the ascending aorta. The intima (arrow) is hyperattenuated due to severe anemia. **(b)** Contrast-enhanced CT scan shows the intimal flap (arrowhead) in the ascending aorta, coarctation (*) in the descending aorta, and substantial collateral circulation through bronchial and intercostal arteries (arrows). Mediastinal hemorrhage and bilateral pleural effusions are also evident.

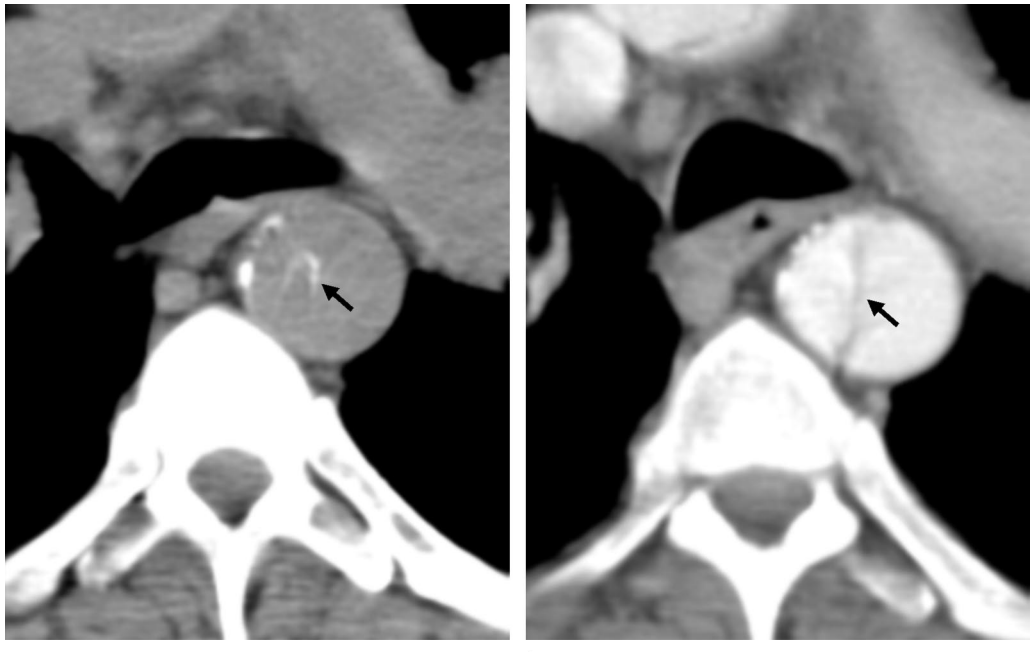

a. b.

Figure 4. Stanford type B typical aortic dissection. **(a)** Unenhanced CT scan depicts displaced intimal calcifications (arrow) in the descending aorta. **(b)** Contrast-enhanced CT scan shows an intimal flap (arrow) in the descending aorta.

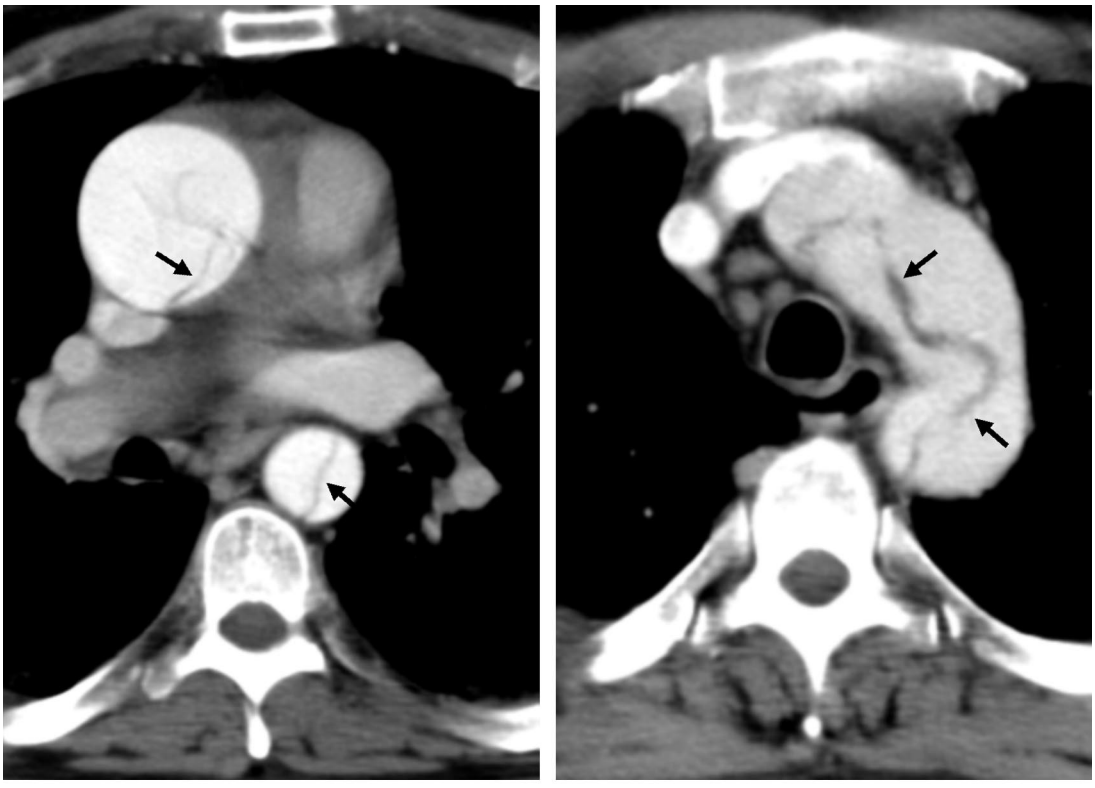

a. **b.**

Figure 6. Contrast-enhanced CT scans of Stanford type A typical aortic dissection show the intimal flaps (arrows) in the ascending and descending aorta **(a)** and the aortic arch **(b)**.

Figure 5. Unenhanced CT scan depicts calcified thrombus (arrow) in the descending aorta, which mimics displaced intimal calcification.

Although hypertension is the most frequent factor predisposing patients to aortic dissection, other conditions also are associated with dissection, including Marfan syndrome and Turner syndrome, other connective tissue diseases, congenital aortic valvular defects, aortic coarctation (Fig 3), aortic aneurysm, infection and other causes of aortitis, and pregnancy (9,10). Cocaine use also has been associated with aortic dissection in otherwise healthy, normotensive patients (11).

Findings at Unenhanced CT

Occasionally, on unenhanced CT scans in aortic dissection, one may see internal displacement of intimal calcifications (Fig 4a). This finding can be problematic because it may be confused with an aneurysm with calcified mural thrombus (Fig 5). High attenuation of the false lumen at unenhanced CT may help the imaging specialist differentiate between the two conditions (12).

Findings at Contrast-enhanced CT

The main finding on contrast-enhanced CT scans of aortic dissection is an intimal flap that separates the true lumen from the false lumen (Fig 3b, Fig 4b, Fig 6). Accurate differentiation at CT between the true and the false lumen was relatively unimportant previously because surgery was the main therapy used; however, this distinction recently has become particularly important for planning endovascular treatment of dissection (13). The slender linear areas of low attenuation that occasionally appear in the false lumen on CT images, known as the cobweb sign, are specific to the false lumen and may aid in its recognition.

a. b.

Figure 7. Stanford type B typical aortic dissection. Sequential contrast-enhanced CT scans show a cobweb sign (arrow)—linear traces of low attenuation—in the false lumen. The beak sign (arrowhead) is caused by a wedge-shaped protrusion of the hematoma in the false lumen. A motion artifact can be seen in the ascending aorta. The true lumen (* in **b**) is compressed and adopts a crescent shape.

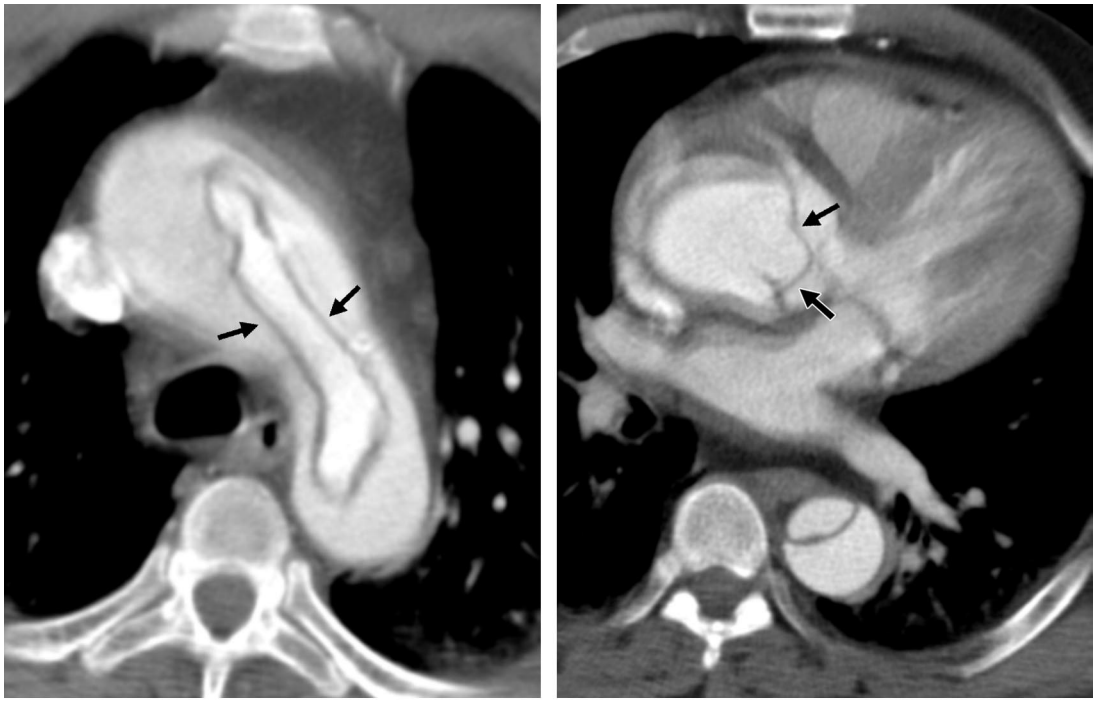

a. b.

Figure 8. Stanford type A typical aortic dissection with intimointimal intussusception. Contrast-enhanced CT scans show the circumference of the intimal intussusception (arrows) in the aortic arch **(a)** and the intimal flap (arrows) in the aortic root **(b)**. Note the intimal flap in the descending aorta in **b**.

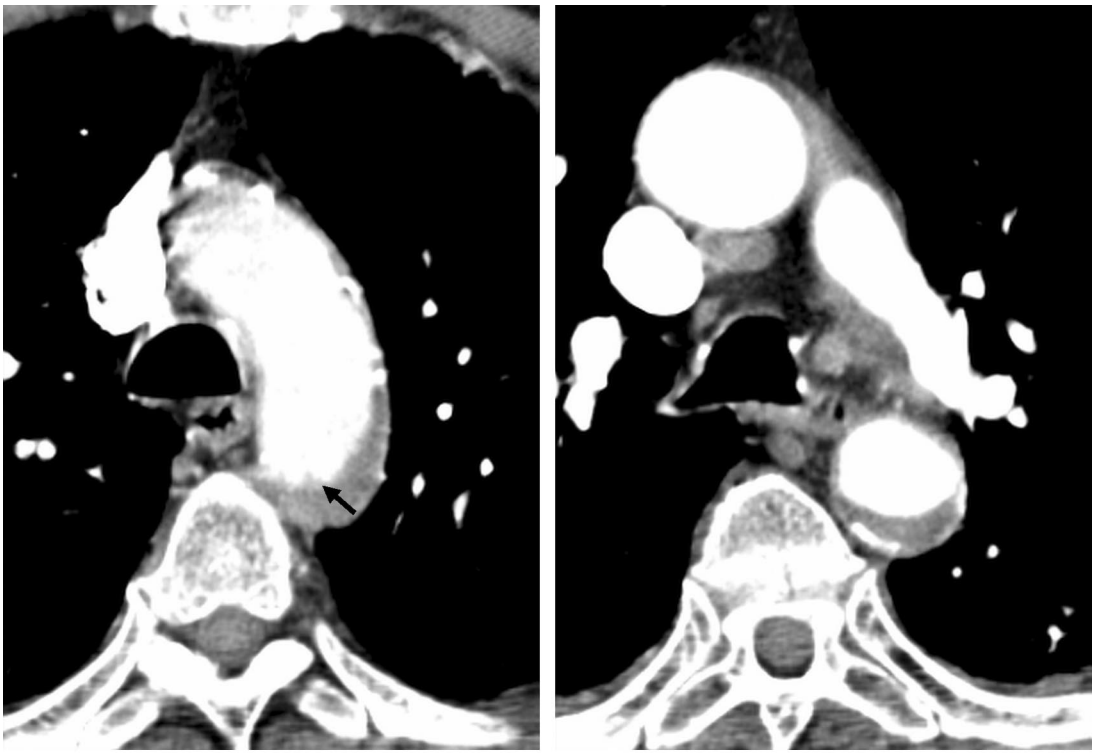

a. b.

Figure 9. Mural thrombus. Sequential contrast-enhanced CT scans show an atheromatous thrombus (arrow in **a**) with an irregular internal border. The thrombus overlies the calcified intima and maintains a constant location in the aorta.

These findings correspond to residual ribbons of the media, incompletely sheared away during the dissection process (14). Two other useful indicators of the false lumen are a larger cross-sectional area and the beak sign. The latter is the cross-sectional imaging manifestation of the wedge of hematoma that cleaves a space for the propagation of the false lumen (Fig 7) (15). On most contrast-enhanced CT scans, however, the true lumen may be identified by its continuity with an undissected portion of the aorta.

Intimointimal intussusception is an unusual type of aortic dissection produced by circumferential dissection of the intimal layer, which subsequently invaginates like a windsock. The intimal tear usually begins near the coronary orifices (Fig 8) (16,17). In intimointimal intussusception, CT scans may show one lumen wrapped around the other lumen in the aortic arch, with the inner lumen invariably being the true lumen.

An aortic aneurysm with intraluminal thrombus may be difficult to distinguish from a dissection with a thrombosed false lumen. The fact that dissection generally has a spiroidal shape, whereas a thrombus tends to maintain a constant circumferential relationship with the aortic wall, can help in visual differentiation between the two. Furthermore, a mural thrombus usually has an irregular internal border, whereas a dissection usually has a smooth internal border. Intimal calcification occurring in an aortic aneurysm is typically located at the periphery of the aorta (Fig 9) (18).

Intramural Hematoma

In contrast to typical aortic dissection, in which there is an intimal tear, IMH is caused by a spontaneous hemorrhage of the vasa vasorum of the medial layer, which weakens the media without an intimal tear (Fig 10) (19).

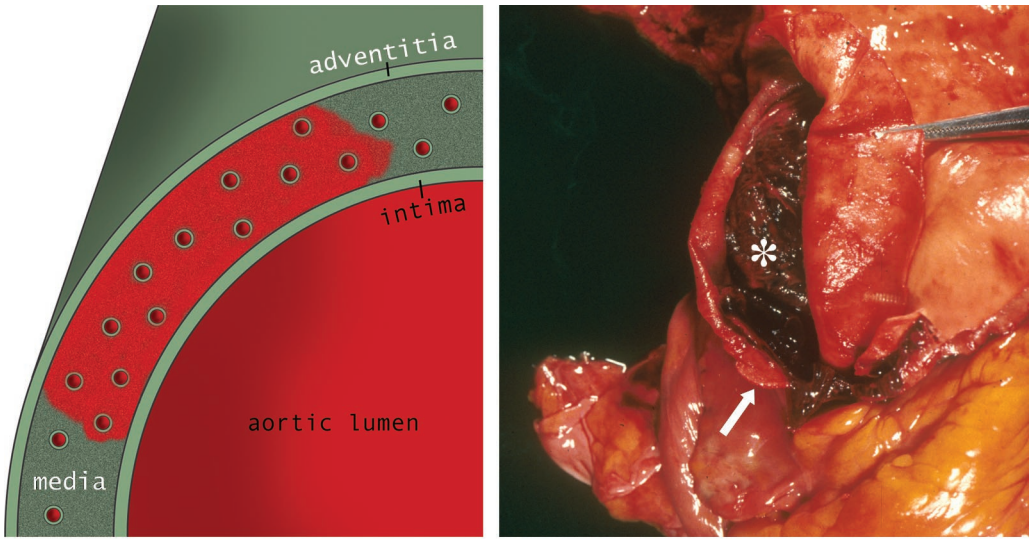

a. b.

Figure 10. **(a)** Schematic of aortic layers in IMH shows a hemorrhage within the media but no intimal tear. Red dots inside the media represent the vasa vasorum. **(b)** Photograph of an autopsy specimen reveals hematoma (*) within the media, between the intima (held in place by a surgical clamp) and the adventitia (arrow). There is no evidence of intimal tear.

The clinical manifestations and the risk factors in IMH are similar to those in typical aortic dissection. IMH accounts for approximately 13% of the prevalence of acute aortic dissection (20).

IMH is commonly classified according to the Stanford system as typical aortic dissection. Many recommend that IMH of Stanford type A be treated surgically (21,22). Some authors have suggested that, in light of the high mortality and morbidity associated with aortic surgery, supportive medical treatment with frequent follow-up imaging may be a rational management option (23,24). Song et al (23) hypothesized that the absence of intimal tear and of continuous flow communication in IMH probably indicate a better clinical outcome than that in typical aortic dissection.

Findings at Unenhanced CT

On unenhanced CT scans, IMH appears as a crescent-shaped area of attenuation in the aortic wall, corresponding to a hematoma in the medial layer. The hematoma may or may not compress the aortic lumen (25). Intimal calcifications also may be displaced by IMH (Fig 11a). It is important to perform unenhanced CT as the first imaging evaluation when aortic dissection is suspected, because contrast material within the vessel may obscure IMH.

Findings at Contrast-enhanced CT

Unlike the false lumen in typical aortic dissection, the crescent-shaped area of IMH remains unenhanced after contrast material administration, and no intimal tear is seen on contrast-enhanced CT scans (Fig 11b). An additional observation that may help differentiate IMH from the thrombosed false lumen in typical aortic dissection is that the latter tends to spiral longitudinally around the aorta, whereas the former tends to maintain a constant circumferential relationship with the aortic wall (18).

Although some have hypothesized that aortic IMH is a precursor to aortic dissection (20,26), the precise relationship between IMH and aortic dissection remains unclear. Several investigators have attempted to assess the usefulness of CT findings for predicting the progression of aortic IMH to aortic dissection. The maximum aortic diameter (≥50 mm), estimated on the basis of the initial CT scan, is predictive of progression in type A IMH (27,28). Findings such as type A IMH, thick hematoma with compression of the true lumen, pericardial effusion, or, less important, pleural effusion were useful for predicting progression to aortic dissection (29). A thicker hematoma may indicate more-active bleeding from the ruptured vasa vasorum, which may result in increased weakening of the intima of the affected aorta (29) (Figs 12, 13).

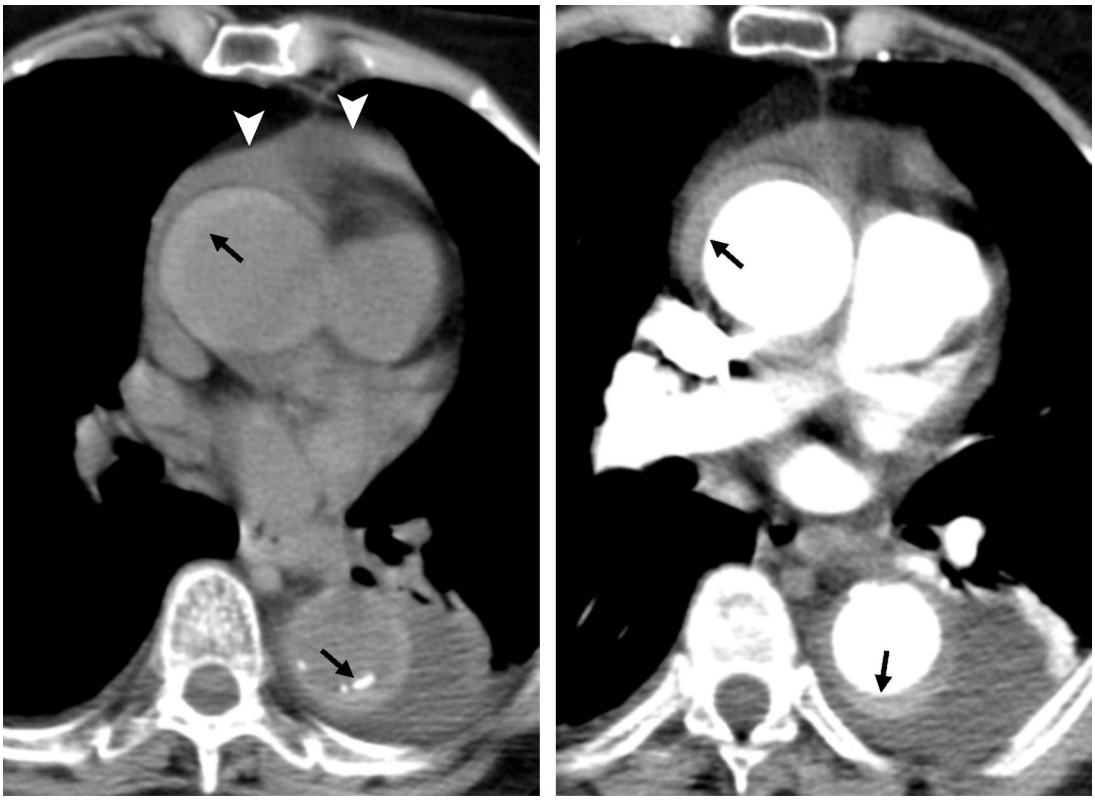

a. b.

Figure 11. Type A IMH. **(a)** Unenhanced CT scan depicts crescent-shaped areas with high attenuation (arrows) extending along the walls of the ascending and descending aorta. The displaced intimal calcifications in the descending aorta indicate a subintimal location. A pericardial effusion (arrowheads) also is visible. **(b)** Contrast-enhanced CT scan shows no enhancement of attenuation in the crescent-shaped areas (arrows). IMH is less apparent here than on the unenhanced CT scan in **a**.

Figure 12. Unenhanced CT scan shows Stanford type B IMH (arrow) compressing the lumen of the descending aorta, as well as pleural effusion. These findings increase the likelihood of the hematoma progressing to dissection. The faint lines in the ascending aorta are artifacts.

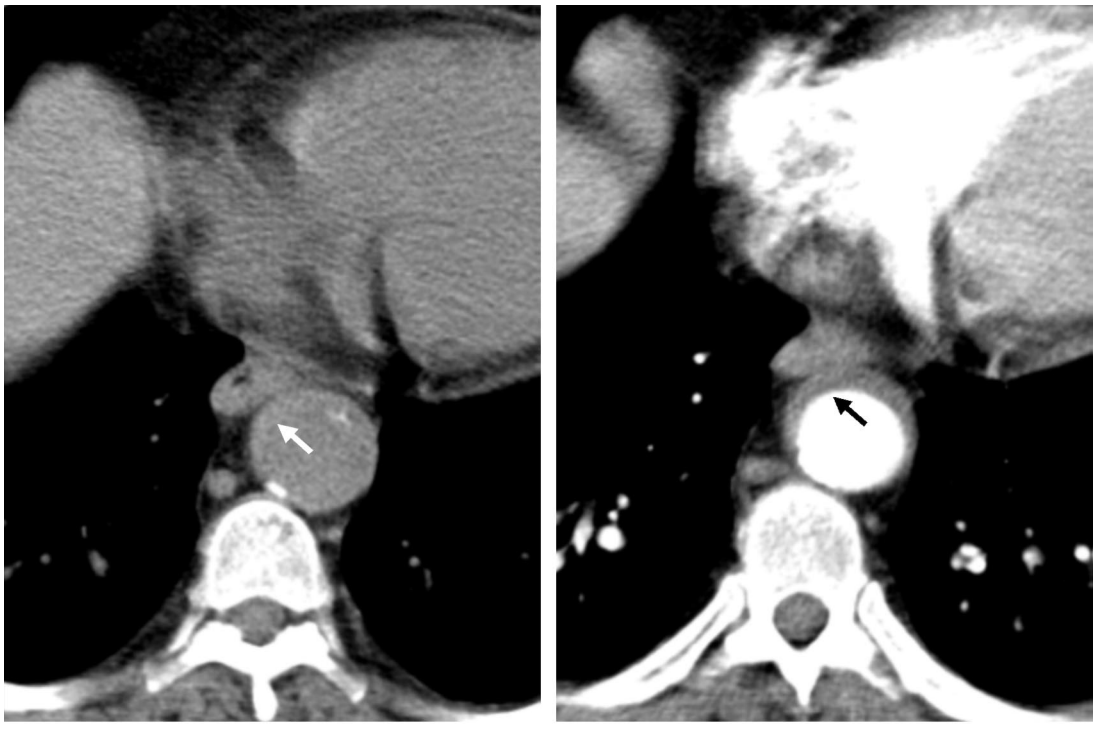

a. b.

Figure 13. Evolution of IMH to typical dissection. **(a)** Unenhanced CT scan shows a crescent-shaped area of high attenuation in the descending aorta, indicating intimal displacement (arrow). **(b)** Contrast-enhanced CT scan acquired at the same time as **a** shows no enhancement of the crescent-shaped area (arrow). **(c)** Contrast-enhanced CT scan acquired 1 week later because the patient reported persistent pain shows aortic dilatation and dissection of the lumen (arrow).

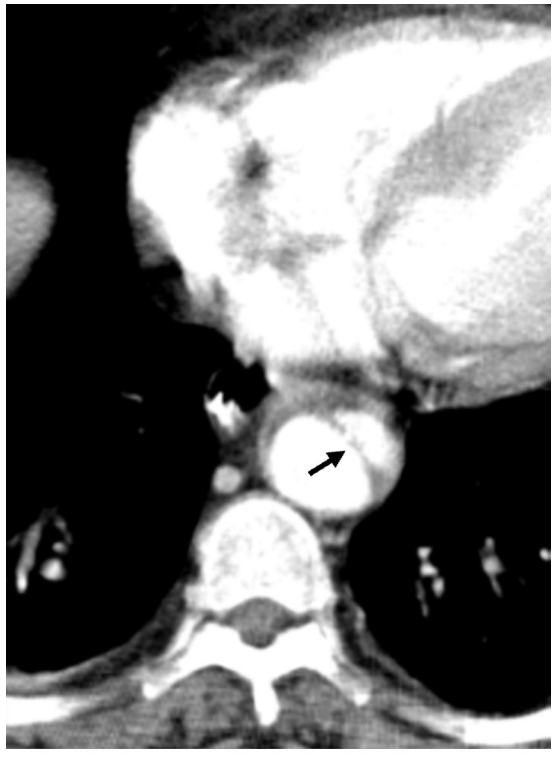

c.

Penetrating Atherosclerotic Ulcer

Penetrating atherosclerotic ulcer is defined as an ulceration of atheromatous plaque that has eroded the inner, elastic layer of the aortic wall, reached the medial layer, and produced a hematoma in the media (30). Involvement of the media can sometimes be complicated by aneurysmal dilatation or, more rarely, rupture (Fig 14). Some authors have theorized that most saccular aneurysms are caused by a penetrating atherosclerotic ulcer (Fig 15) (31–33).

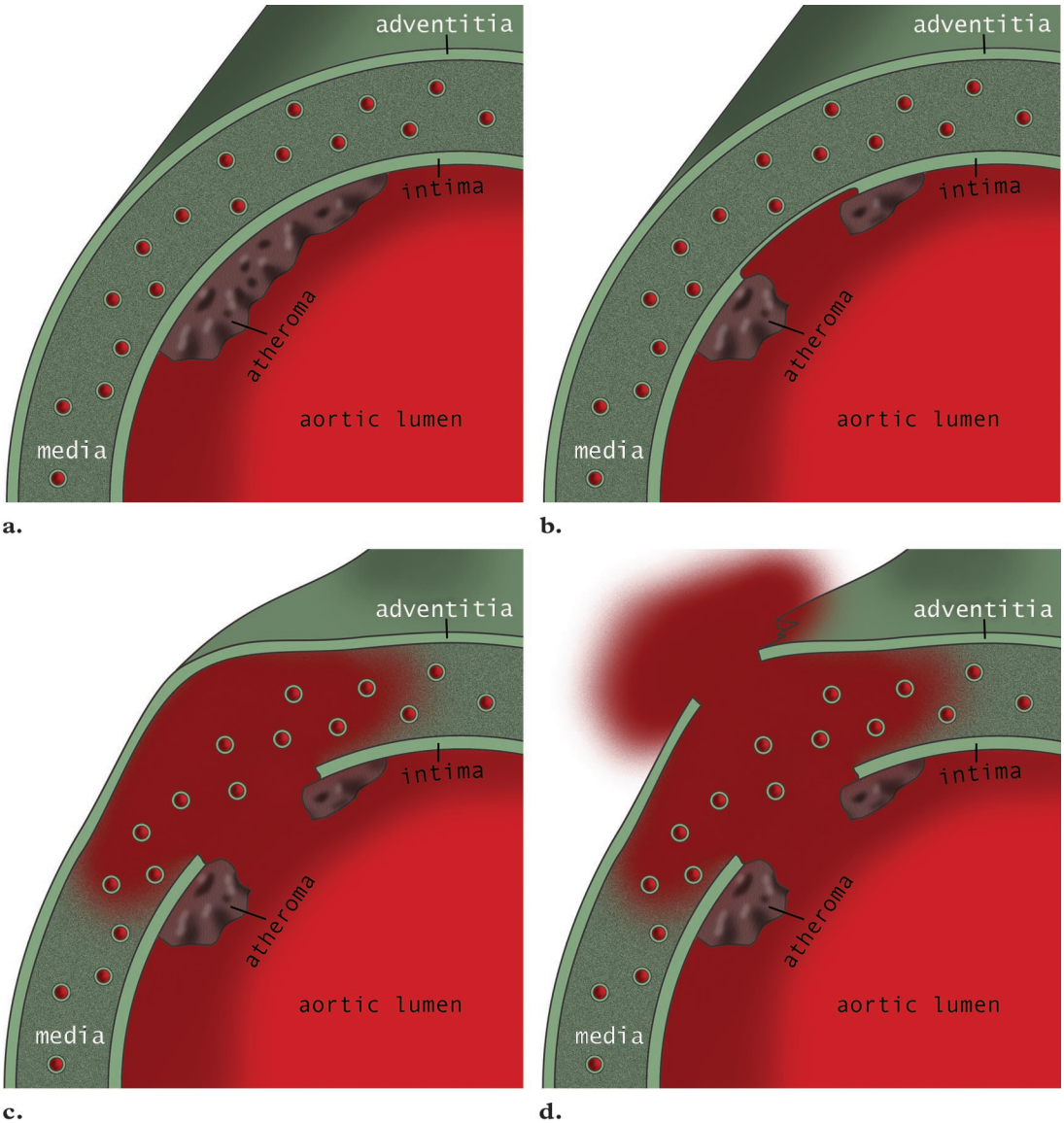

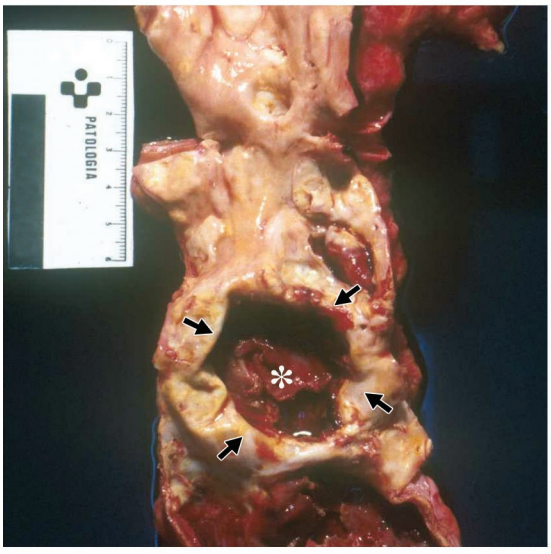

Figure 14. **(a–d)** Diagrams illustrate the four stages in the formation of a penetrating atherosclerotic ulcer: aortic atheroma **(a)**, benign intimal plaque ulceration contained in the intima **(b)**, medial hematoma with potential adventitial false aneurysm **(c)**, and transmural rupture **(d)**. **(e)** Photograph of an autopsy specimen shows severe atherosclerotic changes in the descending aorta, with ulceration of the media (arrows) and IMH (*). Scale is in centimeters.

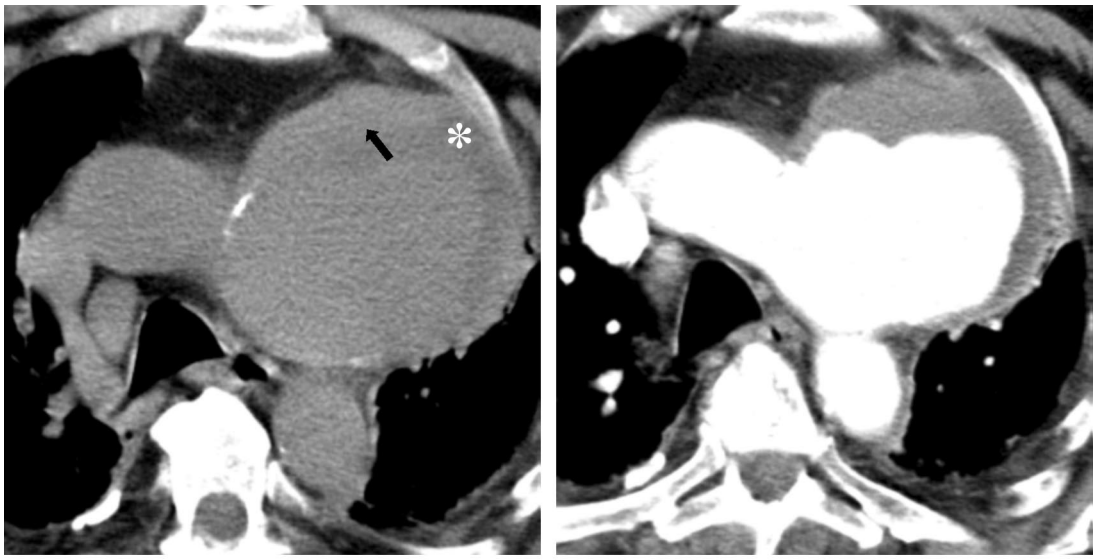

a. b.

Figure 15. Saccular aneurysm in the aortic arch caused by a penetrating atherosclerotic ulcer. **(a)** Unenhanced CT scan shows saccular dilatation of the aortic arch, thrombus (*), and IMH (arrow). **(b)** Contrast-enhanced CT scan shows outflow of contrast material from the aortic lumen.

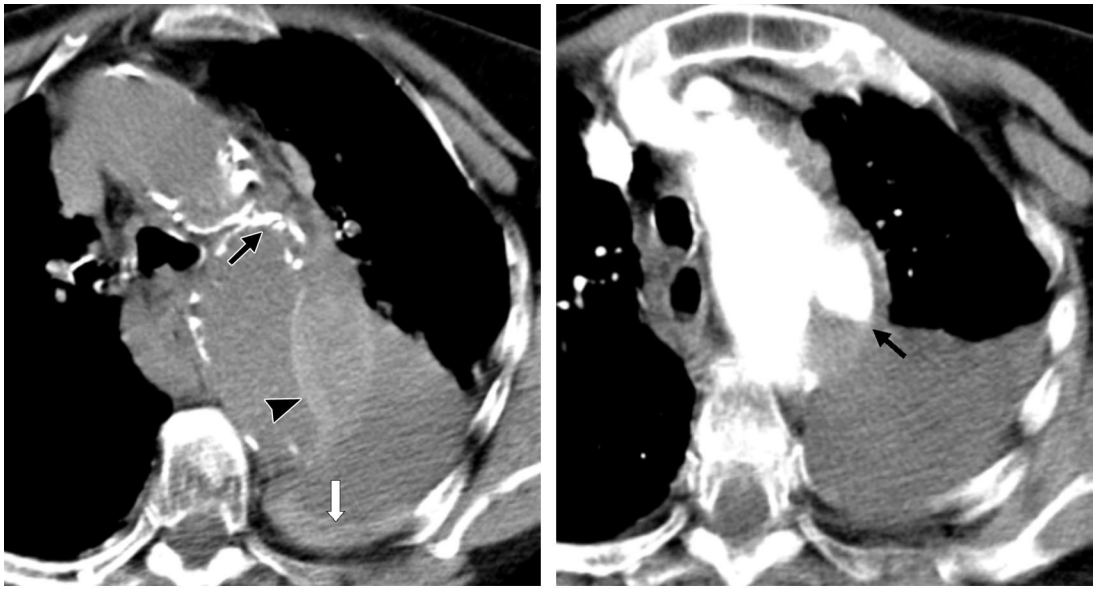

a. b.

Figure 16. Rupture of penetrating atherosclerotic ulcer. **(a)** Unenhanced CT scan of the aortic arch shows an atherosclerotic aorta with displaced intimal calcifications (black arrow), subintimal hematoma (arrowhead), and hemothorax (white arrow). **(b)** Contrast-enhanced CT scan shows the ulcerated aortic lesion and outflow of contrast material from the aortic lumen (arrow).

Unlike typical aortic dissection, penetrating atherosclerotic ulcers most often occur in elderly patients with severe underlying atherosclerosis. These ulcers typically involve the aortic arch and descending thoracic aorta and occur rarely in the ascending aorta, where rapid blood flow from the left ventricle provides protection against atherosclerosis (34).

As for type B typical aortic dissection, the most widespread treatment for penetrating atherosclerotic ulcers is medical therapy. Surgery is performed in patients who have hemodynamic insta-

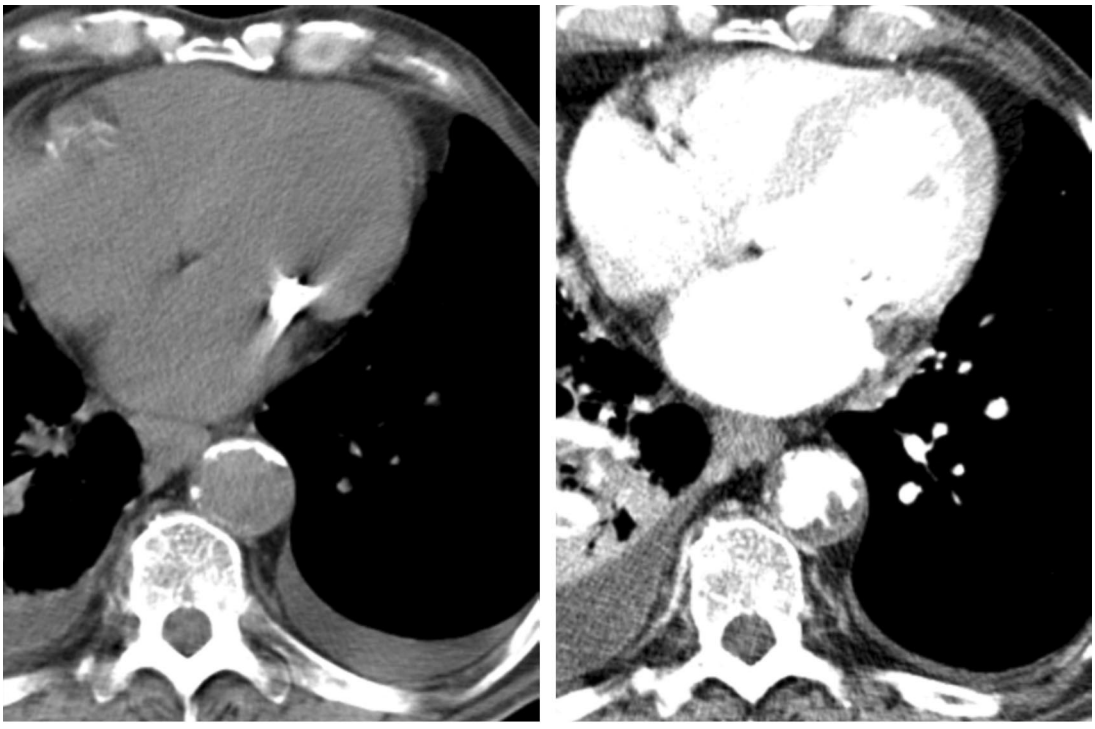

a. b.

Figure 17. Suspected pulmonary thromboembolism in a patient without pain. **(a)** Unenhanced CT scan shows atheromatous changes in the descending aorta but no evidence of IMH. **(b)** Contrast-enhanced CT scan shows multiple ulcerlike lesions.

bility, persistent pain, aortic rupture, distal embolization, or rapid enlargement of the aortic diameter. It is important to emphasize that surgical repair of a penetrating atherosclerotic ulcer is generally more complex and extensive than surgical repair of type B typical aortic dissection; much of the aortic wall may have been damaged by ulceration and may have to be replaced. Aortic dissection, in contrast, usually can be treated with a graft at the site of the proximal intimal tear (30,33–35). Consequently, aortic grafting for penetrating atherosclerotic ulcer may be associated with higher morbidity (eg, increased risk of paraplegia) because of a greater compromise of the spinal cord blood supply during surgery (33).

Findings at Unenhanced CT

In penetrating atherosclerotic ulcer, extensive atherosclerosis and IMH of variable extent are visible on unenhanced CT scans. Frequently the IMH is focal because of medial fibrosis caused by atherosclerosis (34). Displaced intimal calcifications also are often seen (Fig 16a).

Findings at Contrast-enhanced CT

On contrast-enhanced CT scans of penetrating atherosclerotic ulcer, a collection of contrast material is seen outside the aortic lumen (Fig 16b). The appearance of the lesion is similar to that of a peptic ulcer. Lesions can be single or multiple. Penetrating atherosclerotic ulcer is often associated with thickening of the aortic wall, which appears enhanced (35).

Atheromatous ulcers that are confined to the intimal layer sometimes have a radiologic appearance similar to that of penetrating atherosclerotic ulcer. Therefore, particular care should be taken in making a diagnosis of penetrating atherosclerotic ulcer if the lesions are discovered incidentally in an asymptomatic patient and if associated focal IMH is absent (Fig 17) (36). It has been recommended that patients in whom the finding is incidental should receive the same CT follow-up as those with thoracic aortic aneurysms, because one-third of ulcerlike lesions may progress, resulting in mild intervallic aortic enlargement (32).

When rupture and mediastinal hemorrhage occur, it is nearly impossible to differentiate between a ruptured aneurysm and a complicated atherosclerotic ulcer. In both cases, immediate surgical treatment is required.

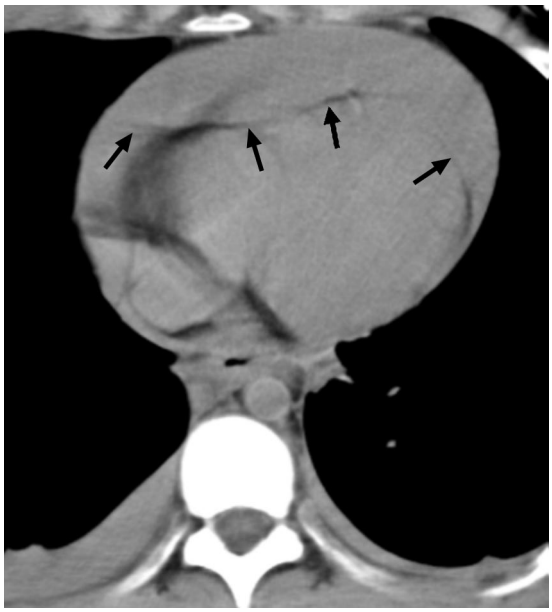

Figure 18. Rupture of Stanford type A typical aortic dissection in a patient with aortic coarctation (same patient as in Fig 3). Unenhanced CT scan shows high-attenuating pericardial effusion (arrows). Note the decreased diameter of the descending aorta.

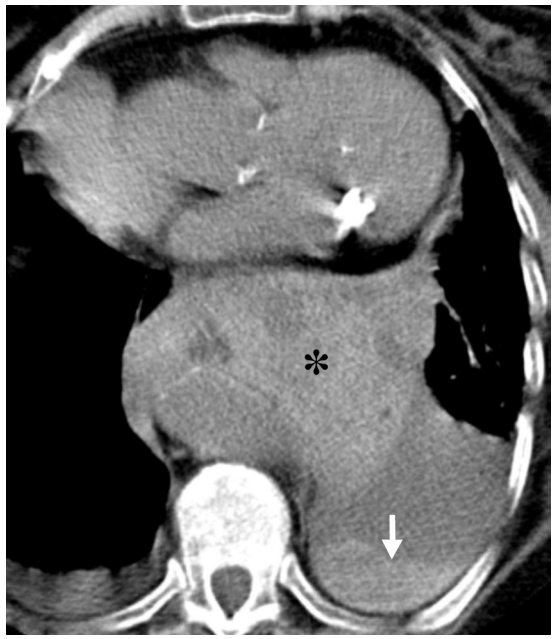

Figure 19. Rupture of penetrating atherosclerotic ulcer. Unenhanced CT scan shows mediastinal hematoma with heterogeneous attenuation, indicating recent bleeding (*). Note the high attenuation of a pleural effusion (arrow), a finding indicative of hemothorax.

Complications

Death from thoracic aortic dissection is usually caused by acute aortic regurgitation, major branch-vessel obstruction, pericardial tamponade, or aortic rupture. Complications arising from thoracic aortic dissection may occur in the thorax or in an extrathoracic location. More than one-third of patients with aortic dissection show signs and symptoms secondary to other organ system involvement. The most common mechanism is the development of ischemia secondary to obstruction of branch arteries originating from the aorta, such as renal arteries. A branch-vessel obstruction could be caused by an extension of the dissection process into the wall of the vessel or a direct compression of the branch artery by an expanding false lumen. Another mechanism of organ system involvement is rupture of the dissected aorta, causing blood to leak into the surrounding structures. Such events are usually fatal (7). It is therefore important in thoracic aortic dissection to evaluate the entire aorta so as to determine the distal extent of the dissection and to detect possible abdominal ischemic disease that might increase morbidity and mortality (3,8).

Hemopericardium, Mediastinal Hematoma, Hemothorax

The risk of fatal aortic rupture in patients with untreated proximal aortic dissection is approximately 90%. Seventy-five percent of ruptures take place in the pericardium, the left pleural cavity, or the mediastinum. The signs of aortic rupture include hyperattenuating mediastinal, pericardial, or pleural fluid collections on unenhanced CT scans (Figs 18, 19) and irregularity of the aortic wall and extravasation of vascular contrast material on contrast-enhanced CT scans.

Rupture of a type A dissection into the pericardial cavity may result in acute pericardial effusion, with a high risk of cardiac tamponade—the most frequent cause of death in patients with this complication. Although the presence of pericardial effusion is not always secondary to a rupture or leak from the dissected aorta, the presence of any pericardial effusion is an ominous sign (7).

Mediastinal Hematoma Dissecting the Sheath of the Pulmonary Arteries

A rare complication of type A aortic dissection is mediastinal hematoma that dissects the sheath of the pulmonary arteries. Blood flows from the ascending aorta to the interstitial space bordering the pulmonary arteries. Rupture usually occurs in the posterior wall of the ascending aorta, adjacent to the right pulmonary artery. Blood seeping from the ruptured aorta can reach the lung through the bronchovascular sheaths (37; Matsuoka Y, unpublished data, March 1999). We have observed two patients with this rare complication (Figs 20, 21).

Figure 20. Rupture of Stanford type A typical aortic dissection. **(a)** Contrast-enhanced CT scan shows stenosis of the pulmonary arteries, which are enveloped in a hemorrhagic sheath. **(b)** Magnified view shows the detail of the stenosis around the left lower lobe pulmonary artery (arrows). **(c)** Scan at lung window setting shows areas of alveolar opacity in the right upper lobe caused by diffusion of blood through the peribronchovascular hilar sheath. **(d)** Posterior view of the autopsy specimen shows hemorrhage in the ascending aorta (arrows) and surrounding the pulmonary arteries (arrowheads). **(e)** Drawing provides a posterior view of the anatomic pathway from the ascending aorta to the pulmonary interstitium.

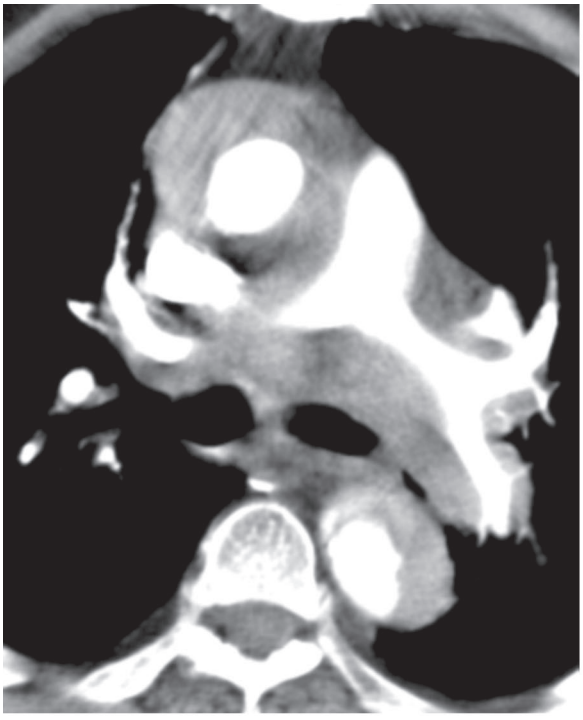

a.

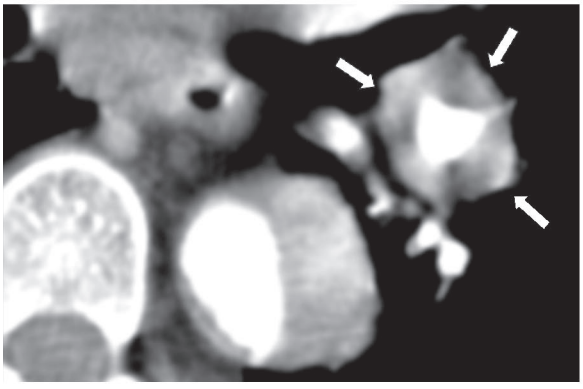

b.

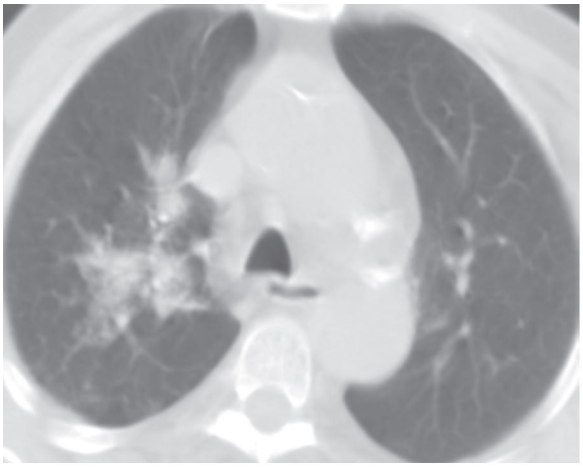

c.

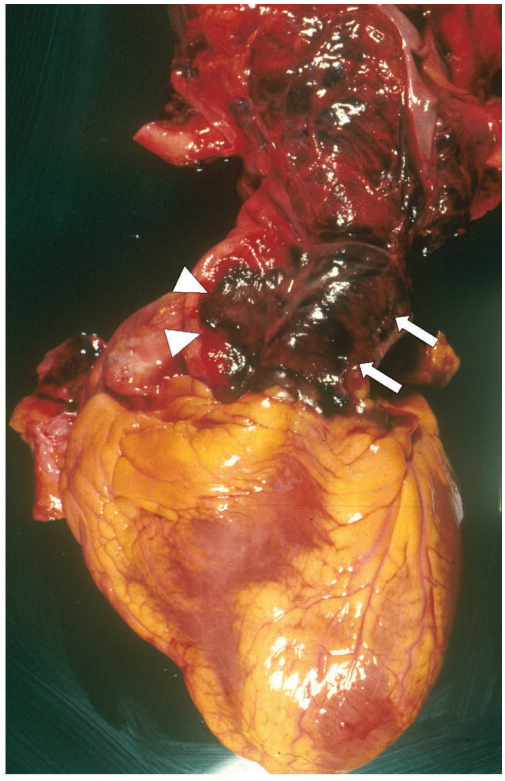

d.

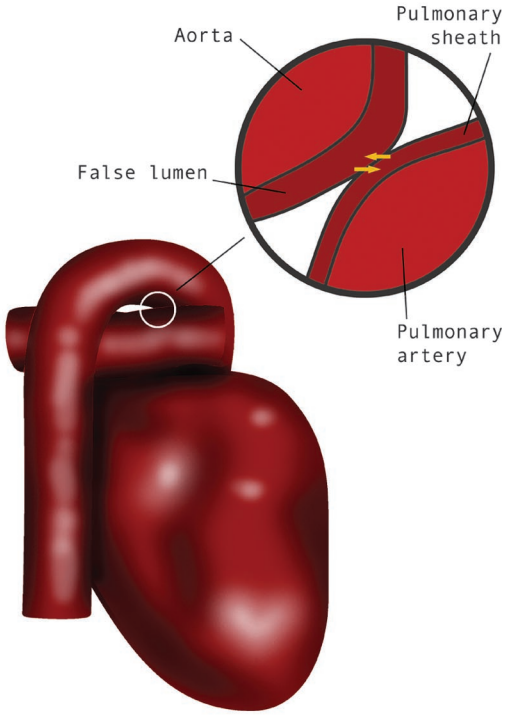

e.

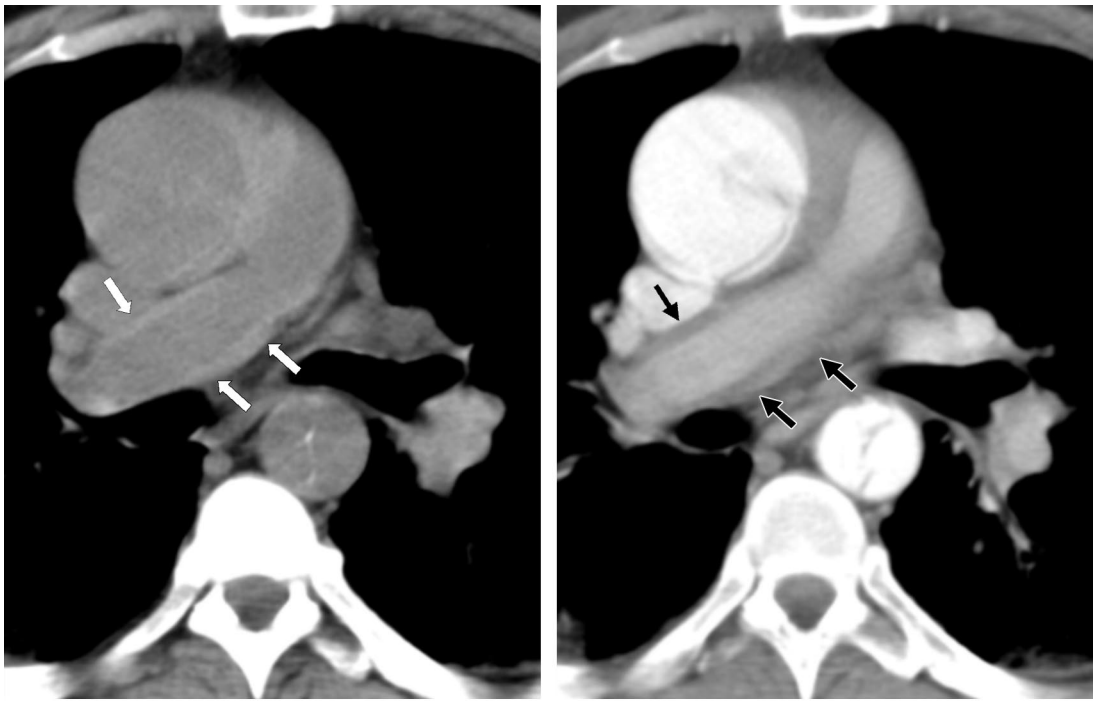

a. b.

Figure 21. Rupture of Stanford type A typical aortic dissection along the sheath of the pulmonary arteries. **(a)** Unenhanced CT scan shows lines of high attenuation along the common trunk and main right pulmonary artery (arrows). **(b)** Contrast-enhanced CT scan shows pulmonary lumen stenosis (arrows). Note the intimal flaps in the ascending and descending aorta.

Neurologic Complications

Cerebral ischemia associated with aortic dissection is caused by supraaortic trunk involvement and is unusual, occurring in only 5%–10% of patients with aortic dissection. If neurologic symptoms are absent, surgical repair is limited to the ascending aorta because aortic arch replacement is associated with a high mortality (Fig 22) (38).

Figure 22. Typical aortic dissection with supraaortic trunk involvement. Contrast-enhanced CT scan shows intimal flaps (arrows) in the innominate trunk and left carotid artery.

Abdominal Complications

Obstruction in the main abdominal arterial branches (celiac, superior mesenteric, renal, and inferior mesenteric arteries) can be demonstrated with contrast-enhanced CT. The frequency of such obstruction has been reported as 27% (39). There are two principal mechanisms of branch-vessel compromise: static, if the dissection flap intersects or enters the branch-vessel origin (Fig 23); and dynamic, if the intimal flap spares the branch vessel but prolapses and covers the branch-vessel origin like a curtain. The shape of the true lumen viewed in cross section on CT scans may be an indicator of possible branch-vessel ischemia: If the true lumen has a crescent shape or is concave to the false lumen (see Fig 7b), there may be a pressure deficit in the true lumen of the aorta and its branches, with a consequent risk of ischemia. The distinction between the two mechanisms of branch-vessel compromise is important because they require different modes of percutaneous treatment. Static obstruc-

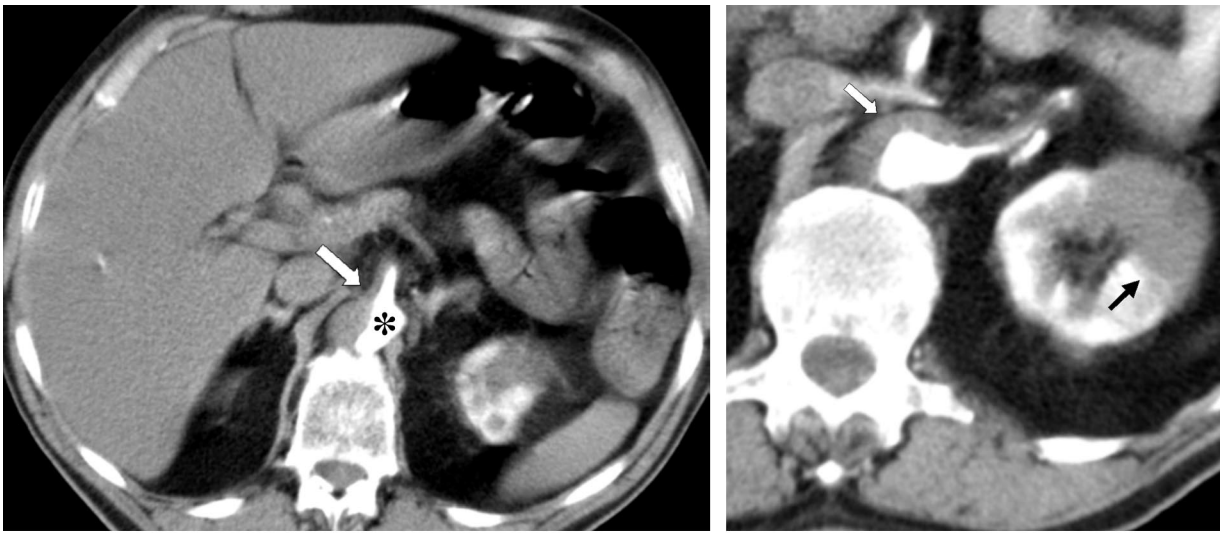

a. b.

Figure 23. Static obstruction of the celiac trunk and right renal artery. **(a)** Contrast-enhanced CT scan shows the intimal flap entering the celiac trunk. The true lumen (*) is narrowed by a thrombotic false lumen (arrow). The liver blood supply is not visible on this arterial-phase image. **(b)** Contrast-enhanced CT scan obtained at a lower level shows the intimal flap (white arrow) entering the left renal artery and producing a left renal infarct (black arrow).

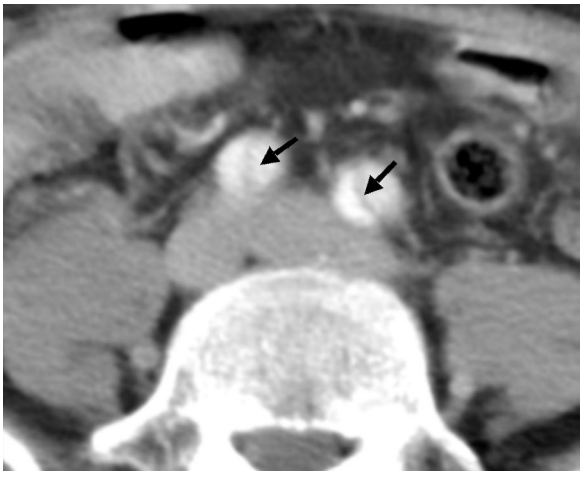

Figure 24. Iliac artery extension from aortic dissection. Contrast-enhanced CT scan shows intimal flaps (arrows) in both common iliac arteries.

tion is treated locally with an intravascular stent. Dynamic obstruction is treated with a fenestration of the intimal flap to decrease pressure in the false lumen (40,41).

Many aortic dissections of type B extend to the iliac arteries without clinical repercussions (Fig 24) (3). If the results of clinical examination suggest ischemia of the legs, that diagnosis can be confirmed with helical CT.

Conclusions

CT should be the first diagnostic test performed when acute aortic dissection is suspected. We believe it is important to perform unenhanced CT first to prevent masking of IMH. Management varies according to classification (Stanford type A or B).

Advances in percutaneous treatment make it important to distinguish between the true lumen and the false lumen; it is essential to know the radiologic findings in typical aortic dissection, IMH, and penetrating atherosclerotic ulcer. Moreover, the entire aorta must be evaluated to determine the extent of the dissection and to identify possible branch-vessel involvement.

Acknowledgments: The authors thank Ricard Valero and Octavio Barbero for technical support, John Giba for linguistic aid, and Kike Fernández for illustrations.

References

1. Demos TC, Posniak HV, Marsan RE. CT of aortic dissection. Semin Roentgenol 1989; 24:22–37.
2. Chung JW, Park JH, Im JG, Chung MJ, Han MC, Ahn H. Spiral CT angiography of the thoracic aorta. RadioGraphics 1996; 16:811–824.
3. Sebastià C, Pallisa E, Quiroga S, Alvarez-Castells A, Dominguez R, Evangelista A. Aortic dissection: diagnosis and follow-up with helical CT. RadioGraphics 1999; 19:45–60.
4. Prete R, Von Segesser LK. Aortic dissection. Lancet 1997; 349:1461–1464.
5. Hirst AE, Johns VR, Klime SW. Dissecting aneurysm of the aorta: a review of 505 cases. Medicine 1958; 37:217–279.
6. Daily PO, Truebold HW, Stinson EB, Wuerfflein RD, Shumway EN. Management of acute aortic dissections. Ann Thorac Surg 1970; 10:237–247.

7. Khan IA, Nair CK. Clinical, diagnostic and management perspectives of aortic dissection. Chest 2002; 122:311–328.
8. Hartnell GG. Imaging of aortic aneurysms and dissection: CT and MRI. J Thorac Imaging 2001; 16:35–46.
9. De Sanctis RW, Doroghazi RM, Austen WG, et al. Aortic dissection. N Engl J Med 1987; 317: 1060–1067.
10. Larson EW, Edwards WD. Risk factors for aortic dissection: a necropsy study of 161 cases. Am J Cardiol 1984; 53:849–855.
11. Fisher A, Holroyd BR. Cocaine-associated dissection of thoracic aorta. J Emerg Med 1992; 10:723–727.
12. Fisher ER, Stern EJ, Godwin JD, Otto CM, Johnson JA. Acute aortic dissection: typical and atypical imaging features. RadioGraphics 1994; 14: 1263–1271.
13. Lee DY, Williams DM, Abrams GD. The dissected aorta. II. Differentiation of the true from the false lumen with intravascular US. Radiology 1997; 203:32–36.
14. Williams DM, Joshi A, Dake MD, Deeb GM, Miller DC, Abrams GD. Aortic cobwebs: an anatomic marker identifying the false lumen in aortic dissection—imaging and pathologic correlation. Radiology 1994; 190:167–174.
15. LePage M, Quint LE, Sonnad SS, Deeb GM, Williams DM. Aortic dissection: CT features that distinguish true lumen from false lumen. AJR Am J Roentgenol 2001; 177:207–211.
16. Nelsen KM, Spizarny DL, Kastan DJ. Intimointimal intussusception in aortic dissection: CT diagnosis. AJR Am J Roentgenol 1994; 162:813–814.
17. Karabulut N, Goodman LR, Olinger GN. CT diagnosis of an unusual aortic dissection with intimointimal intussusception: the wind sock sign. J Comput Assist Tomogr 1998; 22:692–693.
18. Rubin GD. Helical CT angiography of the thoracic aorta. J Thorac Imaging 1997; 12:128–149.
19. Yamada T, Tada S, Harada J. Aortic dissection without intimal rupture: diagnosis with MR imaging and CT. Radiology 1988; 168:347–352.
20. Nienaber CA, von Kodolitsch Y, Peterson B, et al. Intramural hemorrhage of the thoracic aorta: diagnostic and therapeutic implications. Circulation 1995; 92:1465–1472.
21. Murray JG, Manisalli M, Flamm SD, et al. Intramural hematoma of the thoracic aorta: MR imaging findings and their prognostic implication. Radiology 1997; 204:349–355.
22. Rerkpattanapipat P, Jacobs LE, Makornwattana P, Kotler MN. Meta-analysis of 143 reported cases of aortic intramural hematoma. Am J Cardiol 2000; 86:664–668.
23. Song JK, Kim HS, Kang DH, et al. Different clinical features of aortic intramural hematoma versus dissection involving the ascending aorta. J Am Coll Cardiol 2001; 37:1604–1610.
24. Sueyoshi E, Matsuoka Y, Sakamoto I, Uetani M, Hayashi K, Narimatsu M. Fate of intramural hematoma of the aorta: CT evaluation. J Comput Assist Tomogr 1997; 21:931–938.
25. Ledbetter S, Stuk JL, Kaufman JA. Helical (spiral) CT in the evaluation of emergent thoracic aortic syndromes. Radiol Clin North Am 1999; 37:575–589.
26. Mohr-Kahaly B, Erbel R, Kearney P, Puth M, Meyer J. Aortic intramural hemorrhage visualized by transesophageal echocardiography: findings and prognostic implications. J Am Coll Cardiol 1994; 23:658–664.
27. Ide K, Uchida H, Otsuji H, et al. Acute aortic dissection with intramural hematoma: possibility of transition to typical dissection or aneurysm. J Thorac Imaging 1996; 11:46–52.
28. Kaji S, Nishigami K, Akasaka T, et al. Prediction of progression or regression of type A aortic intramural hematoma by computed tomography. Circulation 1999; 100(sII):281–286.
29. Choi SH, Choi SJ, Kim JH, et al. Useful CT findings for predicting the progression of aortic intramural hematoma to overt aortic dissection. J Comput Assist Tomogr 2001; 25:295–299.
30. Stanson AW, Kazmier FJ, Hollier LH, et al. Penetrating atherosclerotic ulcers of the thoracic aorta: natural history and clinicopathologic correlations. Ann Vasc Surg 1986; 1:15–23.
31. Harris J, Bis K, Glover J, Bendick P, Shetty A, Brown O. Penetrating atherosclerotic ulcers of the aorta. J Vasc Surg 1994; 19:90–99.
32. Quint LE, Williams DM, Francis IR, et al. Ulcer-like lesions of the aorta: imaging features and natural history. Radiology 2001; 218:719–723.
33. Levy JR, Heiken JP, Gutierrez FR. Imaging of penetrating atherosclerotic ulcers of the aorta. AJR Am J Roentgenol 1999; 173:151–154.
34. Welch TJ, Stanson AW, Sheedy PF, Johnson CM, McKusick MA. Radiologic evaluation of penetrating aortic atherosclerotic ulcer. RadioGraphics 1990; 10:675–685.
35. Kazerooni EA, Bree RL, Williams DM. Penetrating atherosclerotic ulcers of the descending thoracic aorta: evaluation with CT and distinction from aortic dissection. Radiology 1992; 183:759–765.
36. Hayashi H, Matsuoka Y, Sakamoto I, et al. Penetrating atherosclerotic ulcer of the aorta: imaging features and disease concept. RadioGraphics 2000; 20:995–1005.
37. Panicek DM, Ewing DK, Markarian B, Heitzman ER. Interstitial pulmonary hemorrhage from mediastinal hematoma secondary to aortic rupture. Radiology 1987; 162:165–166.
38. Kouchoukos NT, Dougenis D. Medical progress: surgery of the thoracic aorta. N Engl J Med 1997; 336:1876–1888.
39. Cambria RP, Brewster DC, Gertler J, et al. Vascular complications associated with spontaneous aortic dissection. J Vasc Surg 1988; 7:199–209.
40. Williams DM, Lee DY, Hamilton BH, et al. The dissected aorta. III. Anatomy and radiologic diagnosis of branch-vessel compromise. Radiology 1997; 203:37–44.
41. Williams DM, Lee DY, Hamilton BH, et al. The dissected aorta: percutaneous treatment of ischemic complications—principles and results. J Vasc Interv Radiol 1997; 8:605–625.

This article meets the criteria for 1.0 credit hour in category 1 of the AMA Physician's Recognition Award. To obtain credit, see www.rsna.org/education/rg_cme.html.